

# Hierarchical Alternating Optimization For Enhanced 6DMA-Assisted Over-the-Air Computation

Junjie Gao, Bin Yan, Rui Ma, Zheng Wang, Yongming Huang

*School of Information Science and Engineering*

*Southeast University, Nanjing, China*

Email: junjiegseu@gmail.com, {bin\_yan, ruima}@seu.edu.cn, wznuaa@gmail.com, huangym@seu.edu.cn

**Abstract**—In this paper, an enhanced six-dimensional movable antenna (6DMA) assisted over-the-air computation (AirComp) system is proposed to minimize the computation mean square error (CMSE) in internet of things (IoT) networks. Unlike conventional 6DMA systems, our design not only enables each surface to adjust its 3D position and rotation, but also allows antennas to move within each surface. Specifically, we formulate a joint optimization problem for both enhanced 6DMA configurations and transceiver design. To solve this complicated non-convex problem, we propose a hierarchical alternating optimization (HAO) algorithm which decouples the problem as the subproblems of transceiver design and antennas configuration optimization subproblems. Then, alternating optimization and moth-flame optimization (MFO) are applied to solve them, respectively. Numerical results demonstrate that the proposed enhanced 6DMA scheme significantly outperforms existing approaches.

**Index Terms**—Six-dimensional movable antenna, over-the-air computation, moth-flame optimization.

## I. INTRODUCTION

Over-the-air computation (AirComp) has emerged as a promising paradigm for efficient wireless data aggregation in internet of things (IoT) networks [1]–[3]. Unlike traditional orthogonal access methods, AirComp enables multiple devices to transmit concurrently over the same frequency, achieving simultaneous data transmission and computation with significantly reduced latency and improved spectrum efficiency. However, the performance of AirComp systems may be severely degraded by wireless channel impairments including fading, noise, and signal misalignment.

To address these challenges, various approaches have been explored. In particular, early works mainly focused on transceiver design by optimizing transmit scaling coefficients and receive combining vectors to achieve uniform signal amplitude at the receiver [4], [5]. Recent studies have also integrated intelligent reflecting surfaces (IRS) and amplify-and-forward (AF) relays to enhance the received signal power [6], [7]. Very recently, the emergence of movable antenna (MA) technology has opened new opportunities for dynamic channel optimization, and the related studies have demonstrated the significant performance improvement of both one-dimensional (1D) and two-dimensional (2D) MA arrays [8], [9]. However, these MA configurations are restricted to antenna movements

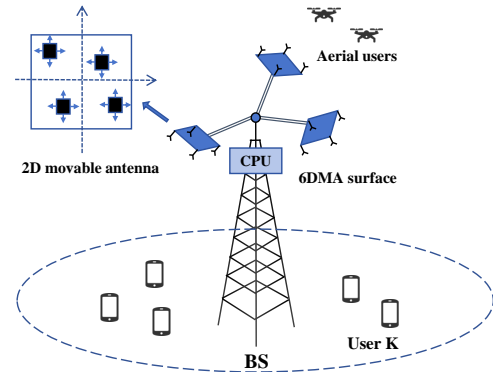


Fig. 1. Enhanced 6DMA-assisted AirComp architecture.

within fixed lines or surfaces. To fully exploit the available spatial degrees of freedom, the six-dimensional movable antenna (6DMA) architecture has been proposed in [10], which maximizes the spatial reconfigurability by enabling antennas surfaces to adjust both three-dimensional positions and rotation angles.

In this paper, we propose an enhanced 6DMA-assisted AirComp system that fully exploits both surface-level and antenna-level mobility. As illustrated in Fig. 1, different from existing 6DMA systems that only adjust surface's position and rotation, our design enables each 6DMA surface to dynamically adjust its 3D position and rotation through controllable telescopic-rotating arms, while simultaneously incorporating movable antennas within each surface. Specifically, the computation mean square error (CMSE) minimization problem is formulated as a unified optimization framework incorporating both antenna configurations and transceiver design. To address it, we propose a hierarchical alternating optimization (HAO) algorithm that consists of two phases: the transceiver design through alternating optimization of transmit coefficients and receive combining vectors, and the antenna configuration update using moth-flame optimization (MFO). Numerical results demonstrate that our proposed approach achieves considerable performance improvement compared to existing schemes.

## II. SYSTEM MODEL

We focus on the uplink transmission of an AirComp system consisting of  $K$  single-antenna users and a BS equipped with

Corresponding author: Zheng Wang (email: wznuaa@gmail.com)

$B$  enhanced 6DMA surfaces. Let  $\mathcal{K} = \{1, 2, \dots, K\}$  and  $\mathcal{B} = \{1, 2, \dots, B\}$  denote the sets of users and enhanced 6DMA surfaces, respectively. Each enhanced 6DMA surface is a uniform planar array (UPA) comprising  $N$  movable antennas, with  $\mathcal{N} = \{1, 2, \dots, N\}$  denoting the antenna index set. The position of the  $b$ -th enhanced 6DMA surface is represented by  $\mathbf{q}_b = [x_b, y_b, z_b]^T \in \mathcal{C} \subset \mathbb{R}^3$  in the global *Cartesian* coordinate system  $o\text{-}xyz$ , where  $\mathcal{C}$  denotes the BS's 3D deployment region. The rotation of surface  $b$  is characterized by  $\mathbf{u}_b = [\alpha_b, \beta_b, \gamma_b]^T$  where  $\alpha_b \in [0, 2\pi)$ ,  $\beta_b \in [0, 2\pi)$ , and  $\gamma_b \in [0, 2\pi)$  denote the rotation angles about the  $x$ -axis,  $y$ -axis and  $z$ -axis, respectively. Within each surface  $b \in \mathcal{B}$ , the  $n$ -th antenna,  $n \in \mathcal{N}$ , can move in a local  $A \times A$  square region  $\mathcal{C}_r$  centered at  $\mathbf{q}_b$ , with position  $\bar{\mathbf{r}}_{b,n} = [\bar{x}_{b,n}, \bar{y}_{b,n}]^T \in \mathcal{C}_r$ .

Meanwhile, we consider a multipath propagation environment between each user and the BS. The channel from user  $k$  to all antennas on the  $b$ -th enhanced 6DMA surface is expressed as:

$$\mathbf{h}_{b,k}(\mathbf{q}_b, \mathbf{u}_b, \{\bar{\mathbf{r}}_{b,n}\}) = \sum_{l=1}^{L_k} \mu_{k,l} \sqrt{g_{l,k}(\mathbf{u}_b)} \mathbf{a}_{b,l,k}(\mathbf{q}_b, \mathbf{u}_b, \{\bar{\mathbf{r}}_{b,n}\}). \quad (1)$$

Here,  $L_k$  denotes the number of propagation paths,  $\mu_{k,l}$  represents the complex path coefficient, and  $\sqrt{g_{l,k}(\mathbf{u}_b)}$  is the effective antenna gain depending on the surface rotation and the direction of arrival (DoA) of the signal [10], [11]. The array response vector  $\mathbf{a}_{b,l,k}$  is given by:

$$\mathbf{a}_{b,l,k} = \left[ e^{-j\frac{2\pi}{\lambda} \mathbf{f}_{l,k}^T \mathbf{r}_{b,1}}, \dots, e^{-j\frac{2\pi}{\lambda} \mathbf{f}_{l,k}^T \mathbf{r}_{b,N}} \right]^T, \quad (2)$$

where  $\lambda$  is the carrier wavelength and  $\mathbf{f}_{l,k}$  is the unit-norm direction of arrival vector:

$$\mathbf{f}_{l,k} = [\cos(\theta_{l,k}) \cos(\phi_{l,k}), \cos(\theta_{l,k}) \sin(\phi_{l,k}), \sin(\theta_{l,k})]^T \quad (3)$$

with azimuth angle  $\phi_{l,k} \in [-\pi, \pi]$  and elevation angle  $\theta_{l,k} \in [-\pi/2, \pi/2]$ . Besides, the global position of the  $n$ -th antenna on the  $b$ -th surface is:

$$\mathbf{r}_{b,n}(\mathbf{q}_b, \mathbf{u}_b, \bar{\mathbf{r}}_{b,n}) = \mathbf{q}_b + \mathbf{R}(\mathbf{u}_b) [\bar{\mathbf{r}}_{b,n}^T, 0]^T, \quad (4)$$

where  $\mathbf{R}(\mathbf{u}_b) \in \mathbb{R}^{3 \times 3}$  is the rotation matrix determined by the rotation angles  $\mathbf{u}_b$  [10].

In the AirComp framework, each user  $k$  holds normalized data  $s_k$  satisfying  $\mathbb{E}[s_k] = 0$ ,  $\mathbb{E}[|s_k|^2] = 1$  and  $\mathbb{E}[s_i s_j^*] = 0$  for  $\forall i \neq j$ . Users simultaneously transmit scaled versions of their data, resulting in the aggregate of received signal:

$$\mathbf{y} = \sum_{k=1}^K \mathbf{h}_k b_k s_k + \mathbf{n}. \quad (5)$$

Here  $\mathbf{h}_k = [\mathbf{h}_{1,k}^T, \dots, \mathbf{h}_{B,k}^T]^T \in \mathbb{C}^{NB \times 1}$  is the overall channel vector from user  $k$  to all  $B$  enhanced 6DMA surfaces based on (1),  $b_k \in \mathbb{C}$  represents user  $k$ 's transmit coefficient and  $\mathbf{n} \sim \mathcal{CN}(0, \sigma^2 \mathbf{I}_{NB})$  is the additive white Gaussian noise (AWGN) vector. Consequently the BS processes the received signal using a combining vector  $\mathbf{w} \in \mathbb{C}^{NB \times 1}$  to produce an estimate:

$$\hat{r} = \mathbf{w}^H \mathbf{y} = \sum_{k=1}^K \mathbf{w}^H \mathbf{h}_k b_k s_k + \mathbf{w}^H \mathbf{n}. \quad (6)$$

### III. PROBLEM FORMULATION

To enhance AirComp performance, our objective is to minimize the distortion between target and estimated function variables which is measured by the CMSE. In particular, based on (6) the CMSE is defined as:

$$\text{CMSE} = \mathbb{E} \left[ \left| \hat{r} - \sum_{k=1}^K s_k \right|^2 \right] = \sum_{k=1}^K |\mathbf{w}^H \mathbf{h}_k b_k - 1|^2 + \sigma^2 \|\mathbf{w}\|^2. \quad (7)$$

The first term represents the signal distortion caused by imperfect channel compensation, while the second term accounts for noise amplification.

To minimize the CMSE in (7), we need to jointly optimize the enhanced 6DMA configurations and transceiver design, leading to the following optimization problem:

$$\min_{\mathbf{q}, \mathbf{u}, \{\bar{\mathbf{r}}\}, \mathbf{b}, \mathbf{w}} \sum_{k=1}^K |\mathbf{w}^H \mathbf{h}_k(\mathbf{q}, \mathbf{u}, \{\bar{\mathbf{r}}\}) b_k - 1|^2 + \sigma^2 \|\mathbf{w}\|^2, \quad (8a)$$

$$\text{s.t. } |b_k|^2 \leq P_c, \quad \forall k \in \mathcal{K}, \quad (8b)$$

$$\mathbf{q}_b \in \mathcal{C}, \quad \forall b \in \mathcal{B}, \quad (8c)$$

$$\|\mathbf{q}_b - \mathbf{q}_j\|_2 \geq d_{\min}, \quad \forall b \neq j \in \mathcal{B}, \quad (8d)$$

$$\mathbf{n}(\mathbf{u}_b)^T (\mathbf{q}_j - \mathbf{q}_b) \leq 0, \quad \forall b \neq j \in \mathcal{B}, \quad (8e)$$

$$\mathbf{n}(\mathbf{u}_b)^T \mathbf{q}_b \geq 0, \quad \forall b \in \mathcal{B}, \quad (8f)$$

$$\bar{\mathbf{r}}_{b,n} \in \mathcal{C}_r, \quad \forall b \in \mathcal{B}, n \in \mathcal{N}, \quad (8g)$$

$$\|\bar{\mathbf{r}}_{b,n} - \bar{\mathbf{r}}_{b,m}\|_2 \geq D, \quad \forall b \in \mathcal{B}, \quad \forall n \neq m \in \mathcal{N}. \quad (8h)$$

Here,  $P_c$  denotes the maximum transmit power,  $d_{\min}$  is the minimum inter-surface distance to avoid mechanical collision,  $D$  is the minimum inter-antenna distance to prevent mutual coupling, and  $\mathbf{n}(\mathbf{u}_b) = \mathbf{R}(\mathbf{u}_b) \bar{\mathbf{n}}$  represents the normal vector of surface  $b$  with  $\bar{\mathbf{n}} = [1, 0, 0]^T$  being the initial normal vector.

More specifically, as for the constraints from (8b) to (8h), (8b) limits each user's transmit power to  $P_c$ , (8c) ensures that each enhanced 6DMA surface remains within the BS deployment region  $\mathcal{C}$ , (8d) maintains a minimum distance  $d_{\min}$  between surfaces to avoid mechanical collisions, (8e) and (8f) prevent mutual signal blockage between surfaces and ensure that surfaces face outward from the BS [10], (8g) and (8h) ensure proper antenna placement within each surface's movement region while maintaining sufficient inter-antenna spacing to avoid mutual coupling.

### IV. THE PROPOSED HAO ALGORITHM

Due to the coupled optimization variables and the complex constraints, the formulated problem in (8a) is highly non-convex. To efficiently solve this problem, we proposed a HAO algorithm that decouples the optimization into two phases:

- Phase 1 (Transceiver Design): For fixed enhanced 6DMA configurations  $(\mathbf{q}, \mathbf{u}, \{\bar{\mathbf{r}}\})$ , we optimize the transmit coefficients  $\mathbf{b}$  and receive combining vector  $\mathbf{w}$  through alternating optimization with closed-form solutions.
- Phase 2 (Enhanced 6DMA Configuration): Optimize enhanced 6DMA configurations  $(\mathbf{q}, \mathbf{u}, \{\bar{\mathbf{r}}\})$  using MFO to

minimize the CMSE subject to constraints, where each configuration's fitness is evaluated through the optimized transceiver design from Phase 1.

### A. Transceiver Design

According to (8a), given the fixed enhanced 6DMA configurations, the optimizing problem of  $\mathbf{w}$  and  $\mathbf{b}$  reduces to:

$$\min_{\mathbf{b}, \mathbf{w}} \sum_{k=1}^K |\mathbf{w}^H \mathbf{h}_k b_k - 1|^2 + \sigma^2 \|\mathbf{w}\|^2, \quad (9a)$$

$$\text{s.t. } |b_k|^2 \leq P_c, \quad \forall k \in \mathcal{K}. \quad (9b)$$

To solve it, we apply the alternating optimization between  $\mathbf{w}$  and  $\mathbf{b}$ :

1) *Optimizing  $\mathbf{w}$  with fixed  $\mathbf{b}$* : Given the transmit coefficients  $\mathbf{b}$ , the optimization of  $\mathbf{w}$  becomes an unconstrained quadratic problem. Taking the derivative of the objective function with respect to  $\mathbf{w}^*$  and setting it to zero, we have

$$\frac{\partial}{\partial \mathbf{w}^*} \left[ \sum_{k=1}^K |\mathbf{w}^H \mathbf{h}_k b_k - 1|^2 + \sigma^2 \|\mathbf{w}\|^2 \right] = 0, \quad (10)$$

which yields the closed-form solution:

$$\mathbf{w}^* = \left( \sum_{k=1}^K |b_k|^2 \mathbf{h}_k \mathbf{h}_k^H + \sigma^2 \mathbf{I}_{NB} \right)^{-1} \sum_{k=1}^K b_k \mathbf{h}_k. \quad (11)$$

2) *Optimizing  $\mathbf{b}$  with fixed  $\mathbf{w}$* : Given the fixed  $\mathbf{w}$ , the optimization problem with respect to  $\mathbf{b}$  is given by

$$\min_{\mathbf{b}} \sum_{k=1}^K |\mathbf{w}^H \mathbf{h}_k b_k - 1|^2 \quad \text{s.t. } |b_k|^2 \leq P_c, \quad \forall k \in \mathcal{K}. \quad (12)$$

Here, for notational simplicity, we define the effective channel  $c_k \triangleq \mathbf{w}^H \mathbf{h}_k = |c_k| e^{j\phi_{c_k}}$  for each user  $k$ . Since each term in the summation involves only a single variable  $b_k$ , the problem in (12) can be decomposed into  $K$  optimization subproblems, which are then solved in a parallel manner. To be more specific, the subproblem for user  $k$  is:

$$\min_{b_k} |b_k c_k - 1|^2 \quad \text{s.t. } |b_k|^2 \leq P_c. \quad (13)$$

Then, by letting  $b_k = |b_k| e^{j\phi_{b_k}}$ , where  $|b_k|$  and  $\phi_{b_k}$  denote the magnitude and phase, respectively, the subproblem in (13) can be rewritten as:

$$\begin{aligned} |b_k c_k - 1|^2 &= |b_k c_k|^2 - 2\text{Re}\{b_k c_k\} + 1 \\ &= |b_k|^2 |c_k|^2 - 2|b_k| |c_k| \cos(\phi_{b_k} + \phi_{c_k}) + 1 \\ &\geq |b_k|^2 |c_k|^2 - 2|b_k| |c_k| + 1 \end{aligned} \quad (14)$$

for any fixed magnitude  $|b_k|$ . Clearly, the minimum of this subproblem is attained when  $\cos(\phi_{b_k} + \phi_{c_k}) = 1$ , such that the optimal phase of  $b_k$  is  $\phi_{b_k}^* = -\phi_{c_k}$ .

With the optimal phase, the subproblem in (13) reduces to magnitude optimization:

$$\min_{|b_k|} (|b_k| |c_k| - 1)^2 \quad \text{s.t. } |b_k|^2 \leq P_c. \quad (15)$$

Note that when  $|c_k| \geq 1/\sqrt{P_c}$ , one can always set  $|b_k|^* = 1/|c_k|$  to achieve zero distortion. On the other hand, when  $|c_k| < 1/\sqrt{P_c}$ , the magnitude should be maximized to  $|b_k|^* = \sqrt{P_c}$  to minimize CMSE. Combined with the optimal phase  $\phi_{b_k}^* = -\phi_{c_k}$ , the optimal transmit coefficient turns out to be:

$$b_k^* = \min \left\{ \sqrt{P_c}, \frac{1}{|c_k|} \right\} e^{-j\phi_{c_k}}. \quad (16)$$

Therefore, for the given antenna configuration, its corresponding transmit coefficient vector and receive combining vector can be alternately optimized in Phase 1 until convergence. Subsequently, the CMSE can be expressed as a function of the enhanced 6DMA configuration  $(\mathbf{q}, \mathbf{u}, \{\bar{\mathbf{r}}\})$ , i.e.,

$$\text{CMSE}(\mathbf{q}, \mathbf{u}, \{\bar{\mathbf{r}}\}) = \sum_{k=1}^K |(\mathbf{w}^*)^H \mathbf{h}_k (\mathbf{q}, \mathbf{u}, \{\bar{\mathbf{r}}\}) b_k^* - 1|^2 + \sigma^2 \|\mathbf{w}^*\|^2. \quad (17)$$

### B. Enhanced 6DMA Configuration Optimization

In this phase, the objective is to optimize 6DMA configuration to minimize the CMSE based on (17). Consequently, the configuration optimization problem is formulated as:

$$\min_{\mathbf{q}, \mathbf{u}, \{\bar{\mathbf{r}}\}} \text{CMSE}(\mathbf{q}, \mathbf{u}, \{\bar{\mathbf{r}}\}) \quad (18a)$$

$$\text{s.t. } (8c), (8d), (8e), (8f), (8g), (8h). \quad (18b)$$

To efficiently solve this problem, the MFO algorithm is employed [12]. In MFO, we initialize  $N_{\text{moth}}$  candidate solutions (moths), where each moth  $M_i$  represents a complete enhanced 6DMA configuration:

$$M_i = [\mathbf{q}^T, \mathbf{u}^T, \text{vec}(\{\bar{\mathbf{r}}\})]^T \in \mathbb{R}^{6B+2NB}. \quad (19)$$

Here,  $\text{vec}(\{\bar{\mathbf{r}}\})$  denotes the vectorized antenna positions within all surfaces. For each candidate, its CMSE can be directly evaluated in Phase 1, given by (17).

Furthermore, in order to evaluate each candidate configuration while ensuring constraint satisfaction, a fitness function is introduced that augments the CMSE with a penalty term:

$$\mathcal{F}(M_i) = \text{CMSE}(M_i) + \tau \cdot |\mathcal{V}(M_i)|, \quad (20)$$

where  $\mathcal{V}(M_i)$  denotes the set of constraint violations. Each element in  $\mathcal{V}(M_i)$  represents a violated constraint:

$$\begin{aligned} \mathcal{V}(M_i) &= \{(\mathbf{q}_b, \mathbf{q}_j) \mid \|\mathbf{q}_b - \mathbf{q}_j\|_2 < d_{\min}, \forall b \neq j \in \mathcal{B}\} \\ &\cup \{(\mathbf{q}_b, \mathbf{q}_j, \mathbf{u}_b) \mid \mathbf{n}(\mathbf{u}_b)^T (\mathbf{q}_j - \mathbf{q}_b) > 0, \forall b \neq j \in \mathcal{B}\} \\ &\cup \{(\mathbf{q}_b, \mathbf{u}_b) \mid \mathbf{n}(\mathbf{u}_b)^T \mathbf{q}_b < 0, \forall b \in \mathcal{B}\} \\ &\cup \{(\bar{\mathbf{r}}_{b,n}, \bar{\mathbf{r}}_{b,m}) \mid \|\bar{\mathbf{r}}_{b,n} - \bar{\mathbf{r}}_{b,m}\|_2 < D, \forall n \neq m \in \mathcal{N}\}. \end{aligned} \quad (21)$$

The penalty parameter  $\tau$  is set sufficiently large to ensure feasible solutions are always preferred. Therefore, moths with lower fitness values represent superior configurations that achieve smaller CMSE and fewer constraint violations.

With the fitness function defined, MFO iteratively updates the moth positions to minimize the fitness function  $\mathcal{F}(M_i)$ . MFO uses a moth-flame mechanism where moths represent current candidate solutions, and flames represent the best positions and serve as attractors. Based on their fitness values,

moths with better performance become flames that guide the movement of other moths. Each moth updates its position by spiraling around its corresponding flame according to:

$$M_i^{(t+1)} = D_i \cdot e^{bl} \cdot \cos(2\pi l) + F_j, \quad (22)$$

where  $D_i = |M_i^{(t)} - F_j|$  is the distance between the  $i$ -th moth and  $j$ -th flame  $F_j$ ,  $b$  is a constant defining the spiral shape, and  $l = (a-1)r+1$  with  $r \sim \mathcal{U}(0, 1)$  being a random variable uniformly distributed over  $[0, 1]$ . The parameter  $a$  decreases linearly over iterations as  $a = -1 - t/T_{\max}$ . This adaptive parameter enables wider exploration initially and closer convergence to flames in later stages. The spiral trajectory contrasts with particle swarm optimization (PSO) algorithm's linear velocity updates, offering better coverage of the search space.

After each moth update, boundary constraints are enforced to ensure that all moths satisfy constraints (8c) and (8g):

$$[M_i]_d = \begin{cases} \max\{-C/2, \min\{[M_i]_d, C/2\}\}, & 1 \leq d \leq 3B, \\ \max\{-A/2, \min\{[M_i]_d, A/2\}\}, & 6B < d, \\ [M_i]_d, & \text{otherwise,} \end{cases} \quad (23)$$

where  $C$  denotes the BS's 3D deployment region for enhanced 6DMA surfaces and  $A$  denotes the local movement region for antennas within each surface.

At each iteration, the flames are updated through a competitive selection process. At iteration  $t$ , we combine the current moth positions with the previous iteration's flames and retain only the best solutions, i.e.,

$$F = \begin{cases} \text{sort}(\{M_i^{(0)}\}), & \text{if } t = 1, \\ \text{best}_{N_{\text{moth}}}(\{M_i^{(t-1)}\} \cup F), & \text{otherwise,} \end{cases} \quad (24)$$

where  $\text{best}_{N_{\text{moth}}}(\cdot)$  selects the  $N_{\text{moth}}$  solutions with lowest fitness values from the combined set. If a moth in the current iteration achieves better fitness than an existing flame, it will replace that flame in the sorted list.

Besides, to balance exploration and exploitation, MFO employs an adaptive flame number strategy:

$$N_{\text{flame}} = \text{round} \left( N_{\text{moth}} - t \cdot \frac{N_{\text{moth}} - 1}{T_{\max}} \right). \quad (25)$$

In early iterations, this strategy allows each moth to follow its own flame, which promotes diverse exploration of the solution space. As iterations progress, more moths are guided by the best flames, thus enhancing local search around promising regions. This adaptive approach avoids the premature convergence commonly observed in PSO, where all particles continuously track the same global best position.

Finally, to summarize, the proposed HAO approach is presented in Algorithm 1. Clearly, we can observe that Phase 2 spans from line 3 to line 18, which constitutes the main MFO iteration loop. Within this loop, Phase 1 is incorporated from lines 13 to 16. As for the complexity, the computational complexity of the MFO algorithm in Phase 2 is  $\mathcal{O}(T_{\max} N_{\text{moth}}(M \log M + M))$  [12] where  $M = 6B + 2NB$  is the dimensionality of each moth. The alternating optimization

**Algorithm 1** Proposed Hierarchical Alternating (HAO) Optimization Algorithm

---

```

1: Initialize  $\{M_i^{(0)}\}_{i=1}^{N_{\text{moth}}}, \mathbf{w}, \mathbf{b}$ 
2: evaluate fitness  $\mathcal{F}(M_i^{(0)})$  for each moth via (20)
3: for  $t = 1$  to  $T_{\max}$  do
4:   update number of flames  $N_{\text{flame}}$  via (25)
5:   update flames  $F$  via (24)
6:   for  $i = 1$  to  $N_{\text{moth}}$  do
7:     if  $i \leq N_{\text{flame}}$  then
8:       update  $M_i^{(t)}$  around  $F_i$  via (22)
9:     else
10:      update  $M_i^{(t)}$  around  $F_1$  via (22)
11:    end if
12:    apply boundary constraints via (23)
13:  repeat
14:    update receive combining vector  $\mathbf{w}$  via (11)
15:    update transmit coefficients  $\mathbf{b}$  via (16)
16:  until the decrement on CMSE is smaller than  $\epsilon$ 
17:  evaluate fitness  $\mathcal{F}(M_i^{(t)})$  via (20)
18: end for
19: end for
20: obtain  $[\mathbf{q}^T, \mathbf{u}^T, \text{vec}(\{\bar{\mathbf{r}}\})^T]^T = F_1$ 
21: return  $\mathbf{q}, \mathbf{u}, \{\bar{\mathbf{r}}\}, \mathbf{w}, \mathbf{b} = 0$ 

```

---

of transceiver design in Phase 1 requires  $\mathcal{O}(J((NB)^3 + KNB))$  operations, where  $J$  is the number of iterations until convergence. Since Phase 1 is embedded within Phase 2 and executed for each moth at every iteration, the overall complexity of the HAO algorithm is  $\mathcal{O}(T_{\max} N_{\text{moth}}(J((NB)^3 + KNB) + M \log(M) + M))$ .

## V. NUMERICAL RESULTS

In this section, we evaluate the performance of the proposed enhanced 6DMA-assisted AirComp system through numerical simulations. We consider a BS deployment region  $\mathcal{C}$  as a cube with side length  $C = 1$  m, equipped with  $B = 3$  enhanced 6DMA surfaces, each containing  $N = 4$  movable antennas. The local antenna movement region is set to  $A = 4\lambda$  with wavelength  $\lambda = 0.125$  m. To avoid mutual coupling, we set the minimum inter-surface distance  $d_{\min} = \frac{\sqrt{2}}{2}\lambda + \frac{\lambda}{2}$  and the minimum inter-antenna distance  $D = \lambda/2$ . The noise power is  $\sigma^2 = -80$  dBm.

For the channel model, we set  $L_k = 4$  paths for each user  $k$ , with path coefficients  $\mu_{k,l} \sim \mathcal{CN}(0, 4 \times 10^{-6})$ . The elevation and azimuth angles of arrival,  $\theta_{l,k}$  and  $\phi_{l,k}$ , are uniformly distributed in  $[-\pi/2, \pi/2]$  and  $[-\pi, \pi]$ , respectively. For the MFO algorithm, we use  $N_{\text{moth}} = 50$  moths, maximum iterations  $T_{\max} = 500$ , spiral parameter  $b = 1$ , penalty parameter  $\tau = 20$ , and convergence threshold  $\epsilon = 10^{-4}$ .

We compare our proposed scheme to the following benchmarks: 1) FPA: A conventional three-sector BS where each sector spans  $120^\circ$  with fixed antenna positions and orientations; 2) 2DMA: The 2D movable antenna array scheme from [9], where antennas can move within each surface but

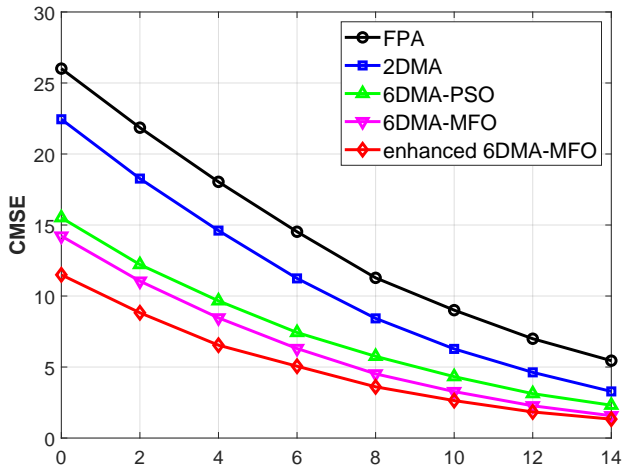


Fig. 2. CMSE versus maximum transmit power  $P_c$  (dBm).

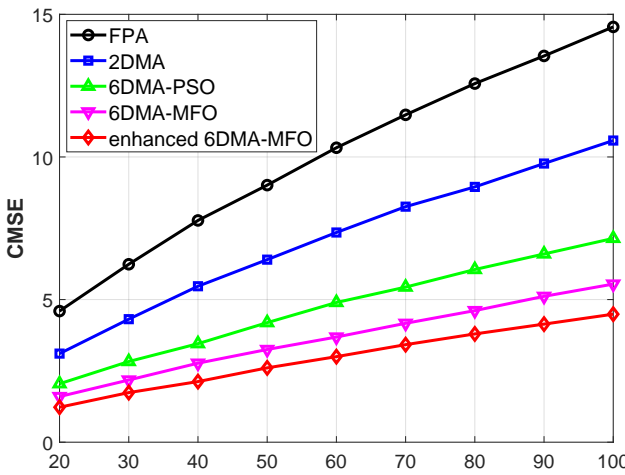


Fig. 3. CMSE versus number of users  $K$ .

surface positions and rotations remain fixed; 3) 6DMA-PSO: The PSO-based 6DMA optimization adapted from [13], where both surface positions and rotations are optimized but individual antenna positions within surfaces are fixed; 4) 6DMA-MFO: The MFO-based standard 6DMA optimization where only surface configurations are optimized without intra-surface antenna mobility.

Fig. 2 illustrates the CMSE performance versus the maximum transmit power  $P_c$  with  $K = 50$ . The proposed enhanced 6DMA-MFO achieves the lowest CMSE, with substantial improvements over the standard 6DMA-MFO (without intra-surface mobility) and 6DMA-PSO schemes. The performance gap is particularly pronounced at lower transmit power levels, where the additional degrees of freedom from antenna-level optimization effectively compensate for limited power resources. Moreover, the MFO-based approaches consistently outperform PSO-based optimization, validating the superior exploration capability of the moth-flame mechanism in the high-dimensional configuration space.

Fig. 3 depicts the CMSE versus the number of users  $K$

with  $P_c = 10$  dBm. As expected, the CMSE increases with  $K$  due to the increased interference and computation load. However, our proposed enhanced 6DMA-MFO scheme maintains superior performance across all user densities, with the performance gap widening as  $K$  increases. This demonstrates the scalability of our approach in dense AirComp networks.

## VI. CONCLUSION

In this paper, we propose an enhanced 6DMA-assisted AirComp system that exploits both surface-level and antenna-level mobility. The developed HAO algorithm, which integrates alternating optimization for transceiver design and MFO for antenna configuration, effectively addresses the non-convex optimization challenge. Numerical results validate the substantial performance gains of the proposed enhanced 6DMA architecture over conventional FPA, 2DMA, and standard 6DMA systems. Future work will explore practical implementation considerations including hardware constraints and extend the framework to multi-cell cooperative scenarios.

## ACKNOWLEDGMENT

This work was supported in part by the National Key RD Program of China under Grants No.2023YFC2205501, and in part by National Natural Science Foundation of China under Grants No.62371124.

## REFERENCES

- [1] B. Nazer and M. Gastpar, "Computation Over Multiple-Access Channels," *IEEE Transactions on Information Theory*, vol. 53, no. 10, pp. 3498-3516, Oct. 2007.
- [2] G. Zhu, J. Xu, K. Huang and S. Cui, "Over-the-Air Computing for Wireless Data Aggregation in Massive IoT," *IEEE Wireless Communications*, vol. 28, no. 4, pp. 57-65, August 2021.
- [3] K. Guo, R. Liu, C. Dong, K. An, Y. Huang and S. Zhu, "Ergodic Capacity of NOMA-Based Overlay Cognitive Integrated Satellite-UAV-Terrestrial Networks," *Chinese Journal of Electronics*, vol. 32, no. 2, pp. 273-282, March 2023.
- [4] W. Liu, X. Zang, Y. Li and B. Vucetic, "Over-the-Air Computation Systems: Optimization, Analysis and Scaling Laws," *IEEE Transactions on Wireless Communications*, vol. 19, no. 8, pp. 5488-5502, Aug. 2020.
- [5] S. Tang, C. Zhang, J. Li and S. Obana, "Miso: Misalignment Allowed Optimization for Multiantenna Over-the-Air Computation," *IEEE Internet of Things Journal*, vol. 11, no. 2, pp. 2561-2572, 15 Jan. 2024.
- [6] T. Jiang and Y. Shi, "Over-the-Air Computation via Intelligent Reflecting Surfaces," *2019 IEEE Global Communications Conference (GLOBECOM)*, Waikoloa, HI, USA, 2019, pp. 1-6.
- [7] S. Tang, H. Yin, C. Zhang, and S. Obana, "Reliable over-the-air computation by amplify-and-forward based relay," *IEEE Access*, vol. 9, pp. 53333-53342, 2021.
- [8] D. Zhang et al., "Fluid antenna array enhanced over-the-air computation," *IEEE Wireless Communications Letter*, vol. 13, no. 6, pp. 1541-1545, June 2024.
- [9] N. Li, P. Wu, B. Ning, L. Zhu and W. Mei, "Over-the-Air Computation via 2-D Movable Antenna Array," *IEEE Wireless Communications Letters*, vol. 14, no. 1, pp. 33-37, Jan. 2025.
- [10] X. Shao, Q. Jiang, and R. Zhang, "6D movable antenna based on user distribution: Modeling and optimization," *IEEE Transactions on Wireless Communications*, vol. 24, no. 1, pp. 355-370, Jan. 2025.
- [11] X. Zhan et al., "Rapid Phase Ambiguity Elimination Methods for DOA Estimator via Hybrid Massive MIMO Receive Array," *Chinese Journal of Electronics*, vol. 33, no. 1, pp. 175-184, January 2024.
- [12] Shehab, M., Abualigah, L., Al Hamad, H. et al. Moth-flame optimization algorithm: variants and applications. *Neural Comput & Applic* 32, 9859-9884, 2020.
- [13] X. Shao, R. Zhang and R. Schober, "Exploiting Six-Dimensional Movable Antenna for Wireless Sensing," *IEEE Wireless Communications Letters*, vol. 14, no. 2, pp. 265-269, Feb. 2025.